ELSEVIER

Nuclear Instruments and Methods in Physics Research A 465 (2001) 482–497

NUCLEAR INSTRUMENTS & METHODS IN PHYSICS RESEARCH Section A

www.elsevier.nl/locate/nima

Multiwire proportional chambers in the HERMES experiment

A. Andreev[a], S. Belostotski[a], G. Gavrilov[a], O. Grebenjuk[a], E. Ivanov[a], A. Kisselev[a], A. Krivchitch[a], S. Kozlov[a], V. Maleev[a], O. Miklukho[a], Yu. Naryshkin[a], S. Patrichev[a], V. Razmyslovich[a], V. Trophimov[a], A. Vassiliev[a], V. Vikhrov[a], E. Cisbani[b,*], S. Colilli[b], S. Frullani[b], F. Garibaldi[b], F. Giuliani[b], M. Gricia[b], M. Iodice[b], M. Lucentini[b], F. Santavenere[b], G.M. Urciuoli[b]

[a] *Petersburg Nuclear Physics Institute, Russian Academy of Science, Gatchina, St. Petersburg district 188350, Russia*
[b] *Physics Laboratory, Istituto Superiore di Sanità and INFN Sezione di Roma-gruppo Sanità, viale Regina Elena 299, Rome, I-00161 Italy*

Received 21 November 2000; accepted 8 February 2001

Abstract

The multiwire proportional chambers of the HERMES spectrometer are described. Each chamber consists of a series anode–cathode planes which measure position along axes at -30°, 0°, and $+30^\circ$ relative to horizontal. The anode wire spacing is 2 mm, while the anode–cathode plane spacing is 4 mm. The chambers are located in the spectrometer magnet gap which imposed strong constraints on their design. A nonflammable gas mixture of Ar(65%), CO_2(30%) and CF_4(5%) is used and an efficiency plateau 500 V wide is obtained. The readout is performed with the LeCroy PCOS4 data acquisition system modified according to the specific requirements of the HERMES experiment. A dedicated water cooling system has been implemented to control and stabilize the surface temperature of the electronic chips mounted on the on-chamber preamplifier boards. A spatial resolution of $\simeq$ 600 μm (rms) per plane has been measured. These chambers are essential for tracking low momentum particles which do not enter the drift chambers after the spectrometer magnet; these particles principally result from the decay of various unstable hadrons. The momentum and angular resolutions in tracking these low momentum particles has been studied and found to be similar to those obtained for high momentum tracks which traverse the entire tracking system of the HERMES spectrometer.

PACS: 29.40.Cs; 29.40.Gx; 07.50.−e

Keywords: Multiwire Proportional Chamber; Compact readout electronics

1. Introduction

In the design of the HERMES spectrometer [1,2] the momentum of a charged particle is derived by the tracking devices (microstrip and

*Corresponding author. Tel.: +39-06-4990-2847; fax: +39-06-4938-7075.

E-mail address: cisbani@iss.infn.it (E. Cisbani).

0168-9002/01/$ - see front matter
PII: S0168-9002(01)00691-X

multiwire drift chambers) located upstream and downstream of a dipole magnet, and external to the high field region. The primary motivation for locating chambers inside the spectrometer dipole magnet (Magnet Chambers—MCs—in the glossary of the HERMES apparatus) was to help resolve multiple tracks in the event reconstruction, by constraining the matching of tracks within the magnet volume as extrapolated from the straight parts of the trajectories measured in the front and rear parts of the spectrometer. It was necessary therefore to design the chambers to be sensitive to particles in the geometrical acceptance of the HERMES spectrometer, i.e., 40 mrad $<|\Theta_{\text{vert}}|<$ 140 mrad and $|\Theta_{\text{horiz}}|<170$ mrad with respect to the interaction point, as well as to take into account the horizontal deflection of the charged particle trajectories by the magnet. Actually the MCs together with the front part of HERMES tracking system are capable of reconstructing the momenta of trajectories without position information from the drift chambers located downstream of the HERMES magnet. This allows the analysis of low momentum particles strongly bent by the magnet, typically the case when studying semi-inclusive reactions which require the detection and tracking of decay products of unstable particles, such as the low momentum pion or proton from Λ hyperon decay.

The requirement of operation in a relatively high magnetic field ($B = 0.8$–1.0 T) has naturally led to the choice of multiwire proportional chambers (MWPC). Since the initial work of Charpak et al. [3], this type of detector has been recognized as a basic tracking and imaging device which works reliably in strong magnetic fields.

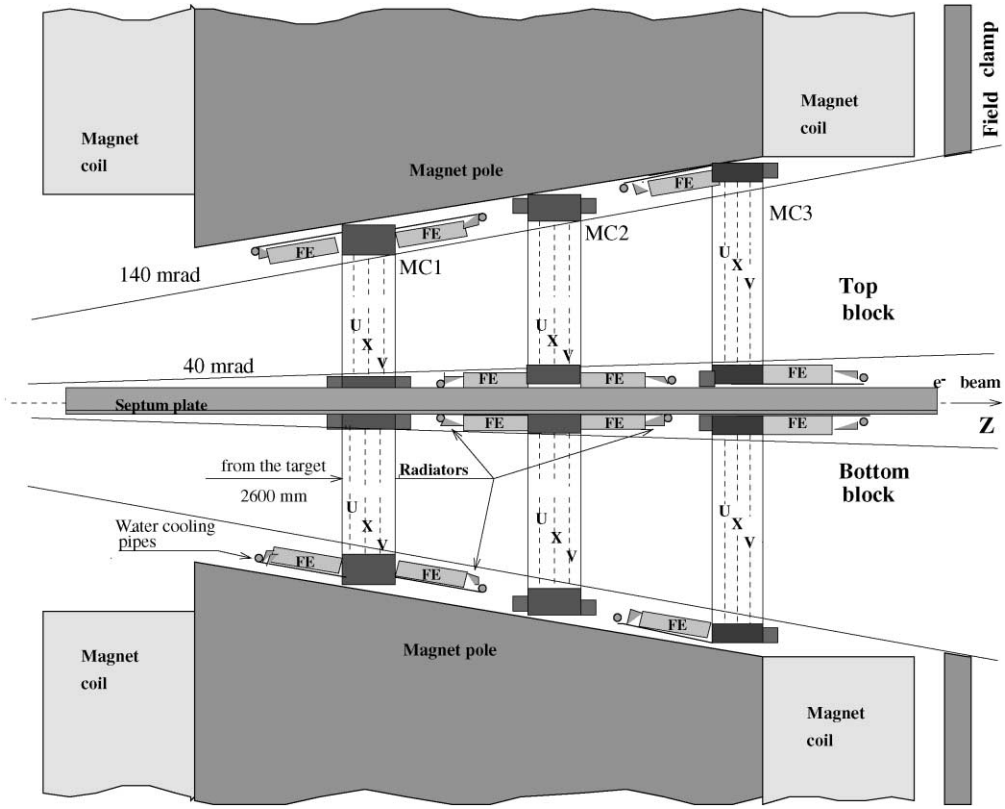

Fig. 1. Side view of the MC set up inside the magnet. FE indicates front-end readout electronics location.

The high efficiency and high rate capability of MWPCs are also necessary for the prescribed tasks of the MCs.

2. Mechanical design

The MCs are mechanically assembled in two blocks (top and bottom) installed in the HERMES spectrometer magnet above and below the septum plate (needed to screen the beam against the magnetic field [1,2]). The plate defines a symmetry plane in the magnet (see Fig. 1). Each MC block consists of three modules MC1, MC2 and MC3.

One MC module contains three anode planes of sense wires U, X, and V interleaved with the cathode wire planes (Fig. 2). The sense wires have a 2 mm spacing and consist of 25 μm diameter gold-plated tungsten. The U and V wires are tilted by $\pm 30^{\circ}$ with respect to the vertical X wires. The cathode planes consist of 90 μm diameter bronze wires with a 0.5 mm spacing. The gap between anode and cathode planes is 4 mm. The principal parameters for the three types of MCs are given in Table 1.

Both anode and cathode electrode frames are made from fiberglass bands glued together with epoxy resin. These frames are sandwiched between two 30 mm thick aluminium frames.

The location of the MCs inside the magnet gap imposed severe constraints on their design. The very limited space between the magnet pole tips and the septum plate, and the requirement of preserving the vertical angular acceptance of the spectrometer required the widths of the frame beams to be reduced. This resulted in substantial frame distortion when tension from the wires was added.

To minimize these distortions, a combination of *inner* and *outer* compensation is applied. The *inner* compensation is accomplished through the cathode planes whose wires are stretched along both the horizontal (4 planes) and vertical (2 planes) directions, but with different tensions per wire: 300 g for horizontal and 150 g for vertical wires, respectively, (see Fig. 3a). Unfortunately, due to the substantial difference in the

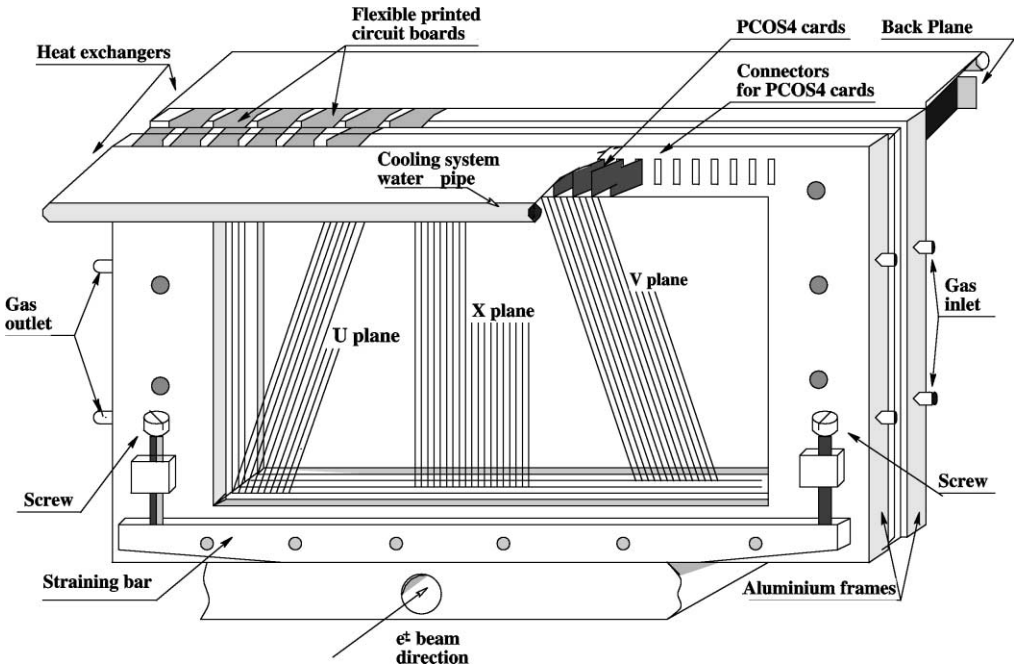

Fig. 2. Layout of one MC module.

Table 1
Mechanical parameters of the MCs

	MC1			MC2			MC3		
Module active area (mm^2)	263 × 996			306 × 1210			347 × 1424		
Sense wire spacing (mm)	2			2			2		
Cathode wire spacing (mm)	0.5			0.5			0.5		
Sense wire ∅	25 μm Au-coated tungsten								
Cathode wire ∅	90 μm Bronze								
Sense wire tension (g)	50–70								
Cathode wire tension (g)	for 4 electrodes—300, for 2 electrodes—150								
	U	*X*	*V*	*U*	*X*	*V*	*U*	*X*	*V*
Sense wires per plane	512	496	512	608	608	608	720	720	720
Front-end boards per module	32	31	32	38	38	38	45	45	45

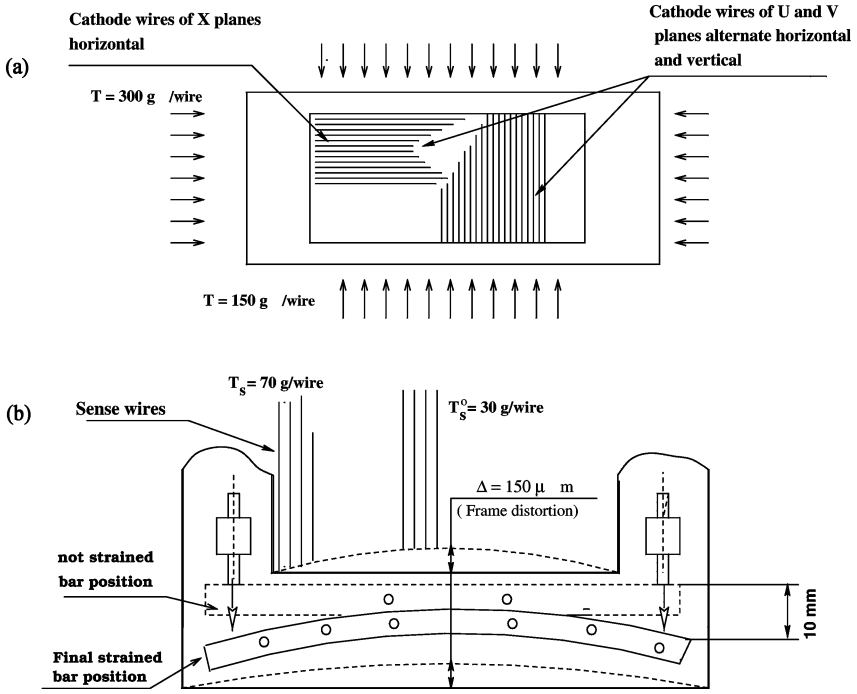

Fig. 3. (a) Scheme of the cathode wire layout and forces applied to the frame. (b) Compensation bar effect on the sense wires tension. T_s^o indicates sense wire tensions corresponding to the unstrained bar position, while T_s is the tension in case of strained bar.

widths and lengths of the vertical and horizontal frame beams, this method only partly helps to maintain the correct MC mechanical configuration. Indeed, the residual force in the module is still sufficient to bend the frame and thereby reduce the sense wire tension from 70 g at both edges of the frame to 30 g in the center (see Fig. 3b).

The residual frame deformations are minimized by an adjustable *outer* compensation system, as shown in Fig. 3b. It includes straining bars embedded in the center of both aluminium frames with two adjusting screws fixed to the frame. In order to eliminate the residual frame deformation of $\Delta = 150$ μm, the bar edges have to be driven down 10 mm by screws.

Fig. 4 shows an example of the sense wire tension T_s distributions for each 10th wire in the MC2 Top and Bottom modules measured in 1998. A wavy character is seen in the tension distributions especially for the U and V planes. This is due to the fact that the sense wires are tilted by $\pm 30^\circ$. It should be noted that in the case of MC3 the straining bars are attached to both horizontal beams, whereas for MC1 (see Fig. 2) and MC2 they are attached to only one of them. Therefore, in the latter case the bends of the opposite narrow beams are not completely compensated.

Nonetheless, Fig. 4 shows that all the wire tension values T_s are within the indicated safe tension range given by

$$T_{crit} \leqslant T_s \leqslant T_L,$$

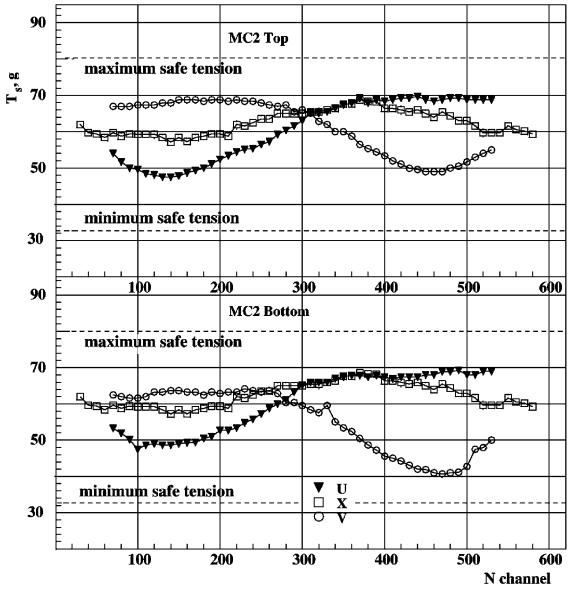

Fig. 4. Wire tensions for MC2 top and bottom modules.

where

$$T_L = T_{elast} - T_{\Delta t^\circ} - T_c.$$

Here T_{elast} is the elastic deformation limit which is in our case 100 g, $T_{\Delta t^\circ}$ is the sense wire tension variation in the temperature range of $\Delta t^\circ = 10$–45°C giving $T_{\Delta t^\circ} = 15$ g, T_c is an additional safety term ($T_c = 5$ g), and T_{crit} is the critical sense wire tension corresponding to the minimum tension needed to retain the sense wires in a plane thereby providing a constant cathode-anode gap. This value is approximately 33 g, depending on the vertical dimension of the chamber.

The sense wire tensions have been examined several times: immediately after fabrication of the chambers in 1994 before their installation in the magnet, during the shutdown late in 1995 and most recently during the 1997/1998 shutdown. All the measurements have been performed at room temperature ($\approx 20^\circ$C). In Table 2 are listed the sense wire tensions for the MC2 Top module, which was disassembled and reassembled during the 1995 shutdown and then inspected again in 1998. No significant changes have been noticed since fabrication, thus confirming that the adopted mechanical design prevents any significant degradation in the frame's mechanical stability.

3. Gas mixture

According to DESY safety regulations, the use of flammable gases for the Magnet Chambers would have required a complex gas system; this, in fact, discouraged the use of a conventional magic gas mixture [4]. Several variants of unflammable gas mixtures were investigated, using a small MC prototype, and their performances were compared

Table 2
Sense wire tensions T_s for MC2 Top and Bottom modules. The construction requirements are $T_{s,min} = 33$ g and $T_{s,max} = 80$ g

Measurement date	X		V		U	
	T_{max}	T_{min}	T_{max}	T_{min}	T_{max}	T_{min}
After fabrication (Aug-94)	72	61	75	57	75	62
Before installation in the magnet (Oct-94)	70	58	72	59.5	71	56.5
Before disassembling (95)	66.8	58	72	55	69	56
After reassembling (Jan-96)	65.3	60.5	72	54.5	68	50
Last inspection (Jan-98)	66.3	58	70	56	68	50

with that of magic gas. Ultimately, we have chosen a mixture of Ar (65%), CO_2 (30%) and CF_4 (5%), the latter component being used as a quencher and aging protector. This mixture provides a gas gain of about 10^5 at the efficiency plateau.

The efficiencies of the chambers have been measured with a collimated ^{90}Sr source of electrons with energies up to 2.28 MeV positioned in front of the chamber and a system of two scintillator counters behind the chamber. The counters detected electrons from the source in coincidence. The threshold electron energy used for tracking was about 1.8 MeV being defined by the thickness of the first scintillator. A mechanical system allowed movement of the chamber in order to investigate the efficiencies at various points.

In Fig. 5, where typical results are shown for the one of the MC3 chambers, these points are numbered as 1–6. The rises of the efficiency curves are very similar, with small differences most likely due to variations in the anode-cathode gap. This small effect corresponds to a gas gain variation of less than 20%.

The efficiency plateau width of 400–500 V, typical for all the chambers, is comparable to that of magic gas mixture.

In order to avoid spurious breakdown, during the experimental runs the chambers operated at a minimal voltage of 2.85 kV, with efficiency close to 100%.The value of the dark current over the whole plateau voltage range is less than 0.5 μA. Since the beginning of data acquisition of HERMES the dark currents and the ionization currents have not shown any tendency to increase, demonstrating that aging effects are negligible.

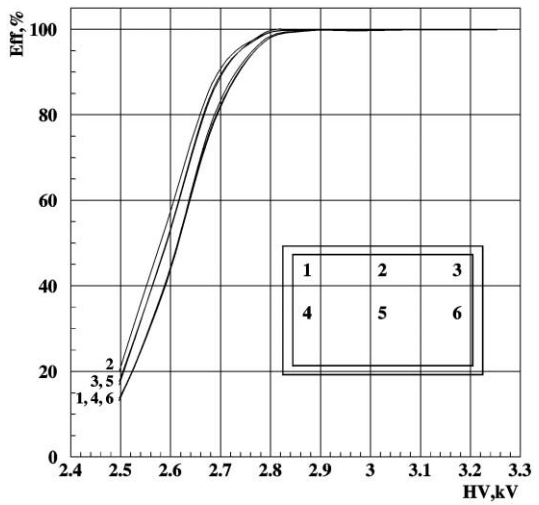

Fig. 5. Efficiencies at various points 1–6 of the MC3 sensitive area, X plane.

4. Readout electronics

The readout of the chambers is performed by the LeCroy PCOS4 acquisition system using a special version developed for the HERMES experiment by LeCroy in collaboration with the Sanità group [5]. This choice has been the consequence of a detailed comparison [6] between three different readout systems: PCOS4, PCOS3 [7] and CROS2 [8].

The main advantages of PCOS4 are:

- good gain (4.3 μV/e) and low noise ($\leqslant$3000e) which allow a lower HV to be used,
- a high data-transfer rate (up to 20 Mbit/s),
- a low readout time (below 18 μs) independent from the total number of channels,
- a reduced number of electronic elements, cabling, and board size,
- fully remotely configurable settings, and
- modularity and flexibility.

Some disadvantages also have to be considered:

- the front-end boards must be powered with three different voltage levels and a common ground,
- extra electronics must be designed to interface the front-end boards to the VME (or CAMAC) data aquisition modules; in PCOS4 jargon this interface is called the ''Backplane''. On the other hand, the presence of the Backplane extends the modularity and flexibility of the PCOS4 system.

The PCOS4 readout chain consists of three main parts: 688 front-end boards (FEs), 48 Backplanes and VME/CAMAC modules (13 dedicated PCOS4 modules and one Programmable Logic Unit). A quite detailed scheme of the MC readout system appears in Fig. 6: the FEs and the

Backplanes are located inside the magnet and therefore are accessible only after having removed the MCs from the HERMES spectrometer. This is possible only during a prolonged shutdown of the HERA accelerator (generally every 2 or 3 years), when the HERMES detector may be disassembled. This fact requires the FEs and Backplanes to be highly reliable.

The FEs (LeCroy 2741-16H, the HERMES version of the PCOS4 original board) are mounted on the chamber frames (see Figs. 1 and 2). On each FE, 16 signals coming from 16 chamber wires are independently amplified by 4 LeCroy MQS104A chips (PA), discriminated, delayed and, when a trigger is present, stored on a 16-bit register (by 2 LeCroy MDL108 chips), ready to be transferred to the Backplane electronics. The FE's parameters (threshold, delay, channel enabling) are remotely configurable, and various test capabilities allow one to check the single channel performance at any time.

The Backplane is the interface between the FEs and the VME/CAMAC modules; each Backplane collects data in parallel from the FEs and sends them to these modules or vice versa. It also provides the mechanical and electrical support of the FEs.

The user can (must) define the Backplane features to a large extent. In the first year of HERMES data acquisition (1995), the Backplane suggested by LeCroy was used. This Backplane version, based on serial FE readout, has been revealed to be unreliable. The failure of one

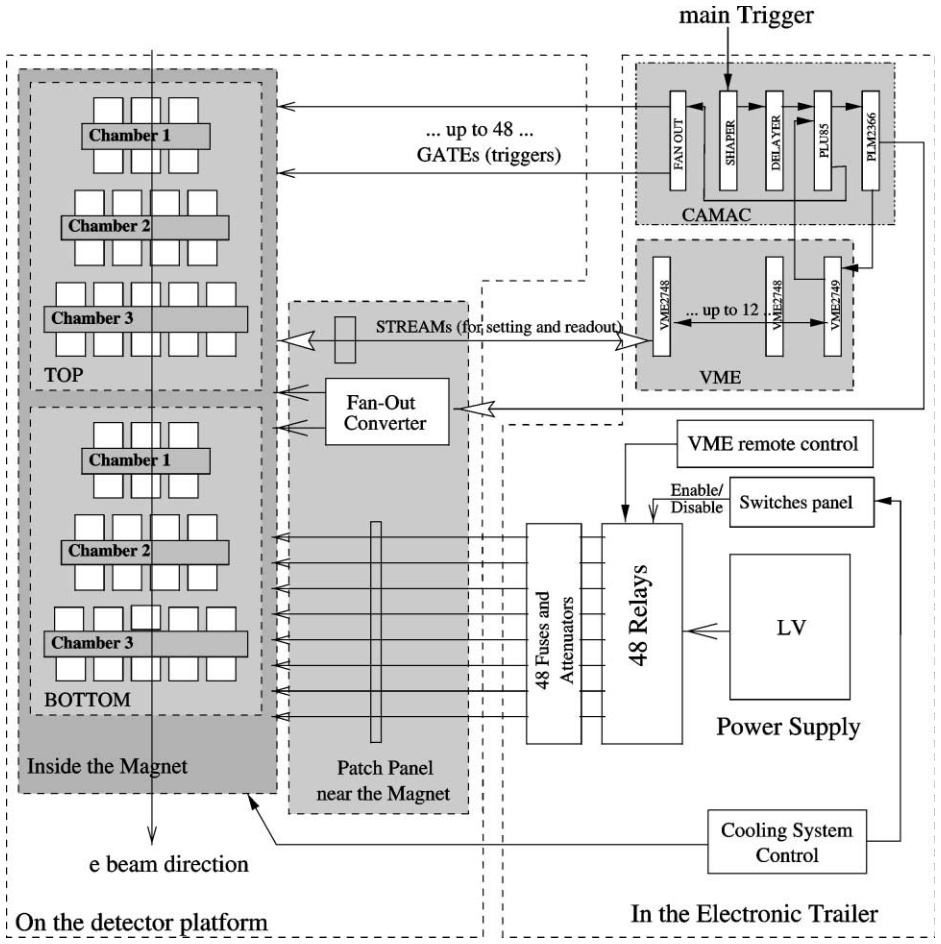

Fig. 6. The MC readout system.

element in the readout chain (one broken chip on one board) compromises the readout of the full Backplane, that is, up to 256 channels. In 1995, this weak point seriously affected the performance of the readout system; a small (8%) percentage of faulty MDL108 chips coming from a damaged batch, which also affected users of PCOS4 at Yale [9], caused a total inefficiency of 48%.

A new, very stable, and reliable Backplane version [6] has been designed in collaboration with LeCroy and manufactured at the Sanità laboratory. It is based on a parallel FE readout which avoids the above mentioned weakness. In the new design, the presence of a faulty element in one board will affect that board only (16 channels instead of 256). The new Backplanes have been operational since June 1996 and have proven to be very reliable, with no significant maintenance required. Electronics failures after this upgrade have caused only a loss of approximately 0.3% of total channels per year.

Data are exchanged between the Backplane and the VME/CAMAC modules via two 8-channel flat cables carrying RS485 and ECL signals at a rate of up to 20 MHz.

The control signals for the Backplanes and FEs are mainly provided by the VME/CAMAC modules, and cause the system to be set in one of four different working modes:

- Configuration mode: before any other operation the various PCOS4 subsystems must be configured proceeding from the VME/CAMAC modules to the Backplanes and to the FEs as well. The settings are performed by the remote HERMES data acquisition (DAQ) computers.
- Calibration mode: in this mode the delays of each FE are tuned by two well separated pulses which simulate the incoming signal and the trigger latch: the precision in the delays is less than 1 ns. This set up must be performed only after the configuration of the FEs and before any attempt at wire chamber data acquisition.
- Acquisition mode: the system is ready to acquire events from the chamber wires.
- Test mode: in this mode the electronic system is tested using internally generated wire signals.

In the acquisition mode, the FEs obtain the signals directly from the chamber wires; these signals are digitized on the FEs. Each FE has 18 bits of data (2 bits for parity check) to transfer over a serial line to the Backplane buffer. This buffer collects in parallel the data from all FEs (upto 16) connected to the Backplane. As soon as this transfer is done the Lecroy VME2748 modules receive, in parallel, the data from the Backplane buffers through the fast (20 MHz) serial links which connect each Backplane to one VME2748. In this way each VME module stores data of 4 Backplanes, that is, 64 FEs or equivalently 1024 wires. The time for all these transfers (readout time) is 17.2 μs and does not depend on the number of channels since all modules and Backplane work in parallel. The total readout time is the sum of this time and the time needed to read the VME modules by the DAQ system.

In this overall scheme, the use of Backplanes and powerful FE electronics reduces the number of cables and of VME/CAMAC modules (and therefore the number of corresponding crates) substantially. A standard readout system commonly needs 16 VME/CAMAC modules (and the related cabling) for 1024 wires, instead of the single module needed in the PCOS4 system.

The trigger logic has been implemented using a programmable logic device (CAEN PLU85) as shown in Fig. 7. During normal readout, Input 1 of the PLU85 is passed to Outputs 1 and 2. The former is the trigger latch (GATE) which is fanned out to the Backplanes (and from there to the FEs); the latter is the READ signal which triggers the Backplane readout.

The trigger logic must take into account the occasional running of the delay calibration procedure, which should be performed from time to time (depending on the required stability of the delay line). At HERMES, the delay calibration is performed at the turn on of the detectors at the beginning of the lepton fill, which lasts 10 hours or so. During this calibration the PLU85 Input 2 is enabled and passed to the Output 1, and from there to the Backplanes and FEs. Other logic is sometimes implemented for testing purposes.

One of the few disadvantages of the PCOS4 system is the necessity of three low voltage (LV)

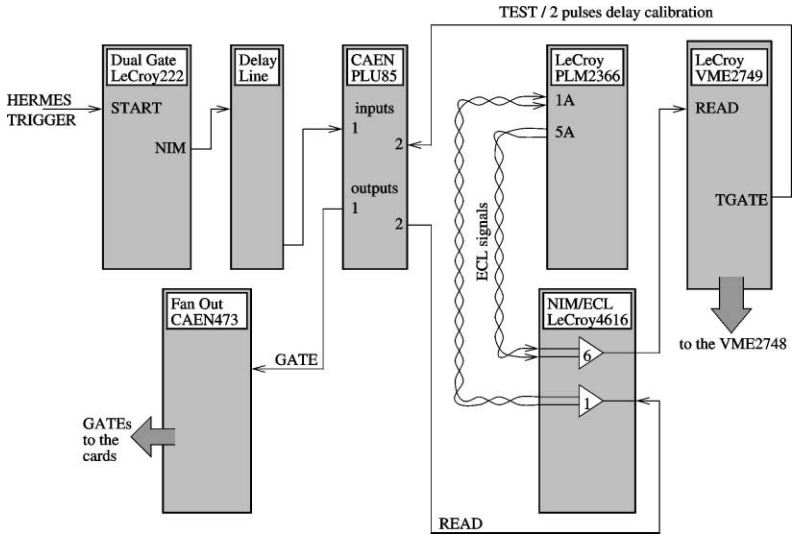

Fig. 7. Logic diagram of the MC trigger.

levels in addition to a common ground in order to power the FEs. In principle each Backplane and the related FEs, should each have three power supplies but to optimize the performance/cost ratio one power supply module energizes more then one Backplane: 12 Backplanes for each -5 V supply, 6 for each 7 V supply, and 4 for each 12 V supply. In order to avoid possible noise sources, linear power supplies are used.

For each Backplane 3-channel DC relays were employed in order to switch on the three levels at the same time.For safety reasons, a single Backplane (and the connected FEs) is powered only if the following conditions are fulfilled at the same time: (1) the LV power supply modules must be powered, (2) the relay related to the Backplane must be powered, which requires that the cooling system is working properly via an interlock, and (3) an electronic switch must be closed by the experiment's online computer control system.

5. The cooling system

The PCOS4 FE's and Backplanes are located in a very limited space in the magnet gap (Fig. 1) under conditions with poor air circulation, and in addition, the power consumption of the FE electronics is substantial (see Table 3). Simple calculations showed that a dedicated, powerful cooling system was needed to keep the surface temperature of the electronic chips low and stable.

A so-called "leakless" water cooling system, similar to the one used for the HERMES electronic racks, has been designed for this purpose. The cooling system consists of vacuum pumps, flow regulators, sensors and an electronic control unit, and has been designed to take into account 30 m long pipes and a more than 7 m height difference between the water pump level and

Table 3
The FE and Backplane power consumption for one MC block; each FE needs about 3 W, each Backplane needs on average 5 W

Chamber	Number of FEs	Power consumption (W)
MC1	95	313.5
MC2	114	376.2
MC3	135	445.5
Total	344	1135.2

the upper water tank located on the magnet. The system has three loops of cooling:

- The FE and Backplane heat is transferred by air convection and through a direct mechanical contact with the chips to a copper air–water heat exchanging radiator attached to each MC.
- The heated water from the radiator flows in an internal cooling loop with less than atmospheric pressure, and passes through a water–water heat exchanger. This exchanger is located outside of the magnet gap.
- Externally supplied cooling water at 7–8°C cools the internal loop water down to 22°C in the water–water heat exchanger.

Temperature sensors (AD590s produced by Analog Devices) are installed on the MC radiators at 32 points in order to measure the temperature on the preamplifier chips directly. Two additional sensors are installed to monitor the water temperature in the internal and external loops.

In the HERMES experimental hall, which has an air temperature of 25°C and relative humidity of 75%, water condensation from the ambient air begins at a temperature of 20°C. Hence, it is not only important to prevent the FE from overheating (their temperature must not exceed 50°C), but also important to keep their temperature above the dew point to avoid water condensation inside the magnet, especially in the case that the power to the on-chamber electronics is switched off.

Operation of such a distributed cooling system and temperature stabilization task requires a dedicated control unit. This control unit continuously monitors the temperature sensors, and based on these data it regulates the water flow in the external water line in order to maintain a constant temperature in the internal water cooling loop, as measured directly after the water–water heat exchanger.

In addition to the safeguards provided by the control unit, in the case that overheating is detected, there are alarms which produce signals which are directly transmitted to the LV modules, causing them in turn to be switched off.

The control unit is connected through an RS232 interface to the main online control computer so that all cooling system data are being read out, stored, and used by common slow control system of the HERMES experiment.

Operation over more than 5 years in the experiment has demonstrated the ability of the MC cooling system to provide reliable temperature control, within the range specified by LeCroy Corporation, for the FE electronics mounted on the chambers.

6. Operation and performance of the magnet chambers in the HERMES experiment

The HERMES experiment has collected data resulting from high-energy positron and electron scattering on polarized H, D and ^{3}He and

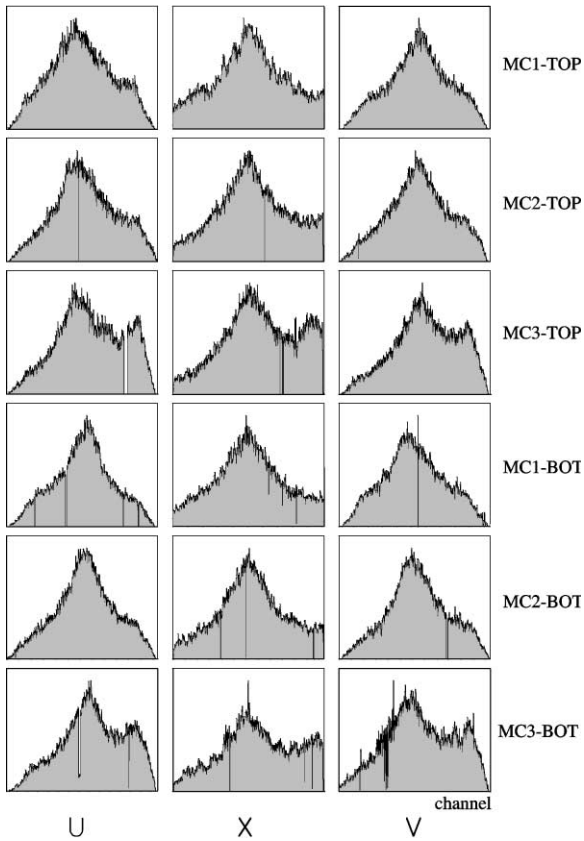

Fig. 8. The MC wire maps; the bumps at the right-hand sides of the spectra come from proton-beam-induced background.

unpolarized gas targets since 1995. Here we focus on the performance of the MCs; the physics results of the HERMES experiment are published elsewhere [10].

The distributions of hits in each wire chamber plane ("wire maps") of the MCs are shown in Fig. 8; the events are from a typical running period of the HERMES experiment. These distributions reflect the angular distribution of the particles produced from the target by the electron(positron) beam, projected on to the coordinate measured by each plane. In the righthand parts of the wire map spectra, a contribution is seen from background related to the proton beam of the HERA collider, which also passes through the septum plate.

Preliminary alignment of the chambers was accomplished using a laser alignment system [2,11]. Final alignment and calibration was performed by analyzing events collected with the spectrometer magnetic field switched off. Assuming straight tracks and minimizing the track residuals, that is, the differences between the measured hit position and the calculated positions, one may determine the relative alignment of the MCs to the tracking detectors upstream and downstream of the magnet. Results from an analysis using data with the magnet switched on are consistent with those found in the minimization procedure just described. The residuals for MC1-3 Top are shown in Fig. 9; all the distributions are well centered, with no deviation of the mean value exceeding 0.2 mm from zero.

Using the residual spectra, the spatial resolution of the MCs can be estimated, and it is found that the rms deviations for all the residual distributions are not more than 850 μm per single plane. A more precise investigation of residual correlations for different MC planes shows that a substantial part of this value comes from the finite accuracy with which the position of the reconstructed tracks is determined with the drift chambers.This detailed analysis gives individual MC plane resolutions of better than 600 μm, which is close to that expected in the ideal case of a uniform track distribution within a 2 mm cell. It has been checked that the MC's spatial resolution is not sensitive to the presence of the spectrometer magnetic field.

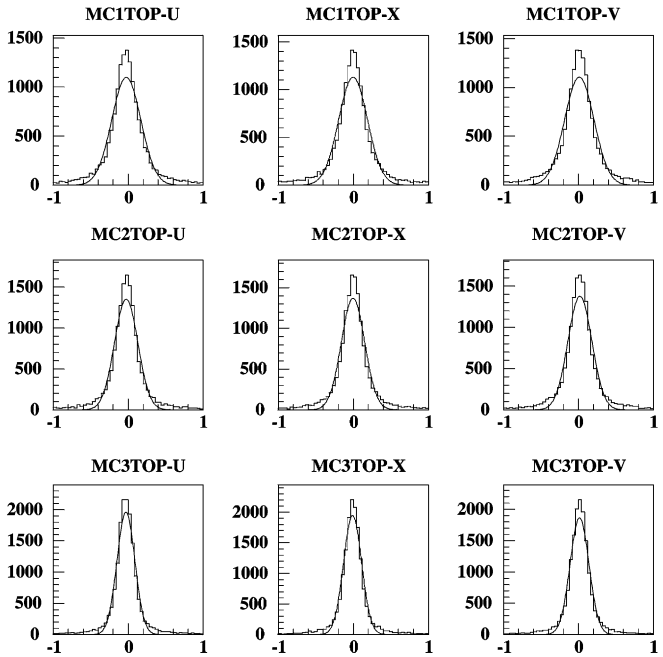

Fig. 9. The distributions of residuals from track position measurements with the TOP block; the units of the abscissae are in cm.

As has been mentioned in the introduction, the MCs are the only means by which to analyze low momentum particles which are bent through sufficiently large angles that they no longer traverse the drift chambers downstream of the spectrometer magnet (so-called "short" tracks). These particles trajectories therefore cannot be reconstructed with the standard HERMES procedure [2,12] which requires tracks to pass through both the front and rear drift chambers (so-called "long" tracks).

Fig. 10 shows a schematic of the HERMES tracking system along with examples of long (full) and short tracks. The front part of the tracking system [2] comprises a vertex chamber (VC), a drift vertex chamber (DVC), and two front chambers (FC); the rear part consists of two sets of back chambers (BC).

The momentum and angular resolutions of reconstruction of short and long tracks in the HERMES tracking system have been studied using "residual" distributions calculated by taking the difference between randomly generated tracks and reconstructed values. The HERMES Monte Carlo program was used to perform the calculation; it uses the CERN library GEANT3 [13] with a database containing the full geometry and composition of the components of the spectrometer. The simulations were made for low momentum pions; the results for short and long tracks are compared in Fig. 11. The track resolutions are calculated for two variants of front tracking reconstruction: the standard method of using DVC (or VC) and FC, and the method of using the FC only [2, Section 5.6.3]. In the momentum range considered, the different methods give very similar results for long tracks, however, for short tracks the difference between the two methods is substantial. The tracking is clearly better if all the chambers in the front region are used in the reconstruction of short tracks, giving momentum resolution and angular resolutions very close to the values found for long tracks.

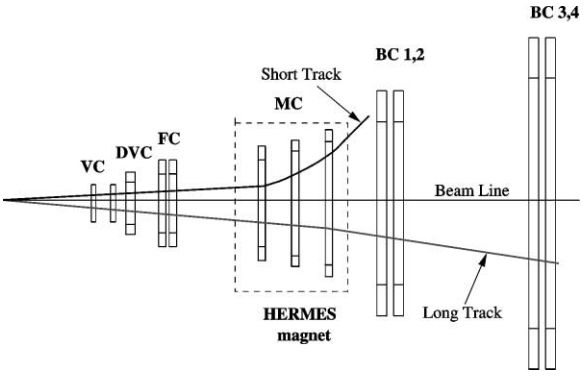

Fig. 10. Scheme of the HERMES tracking system (top view). One long track (crossing all the tracking chambers) and one short track (going out of the tracking system before BC1) are shown.

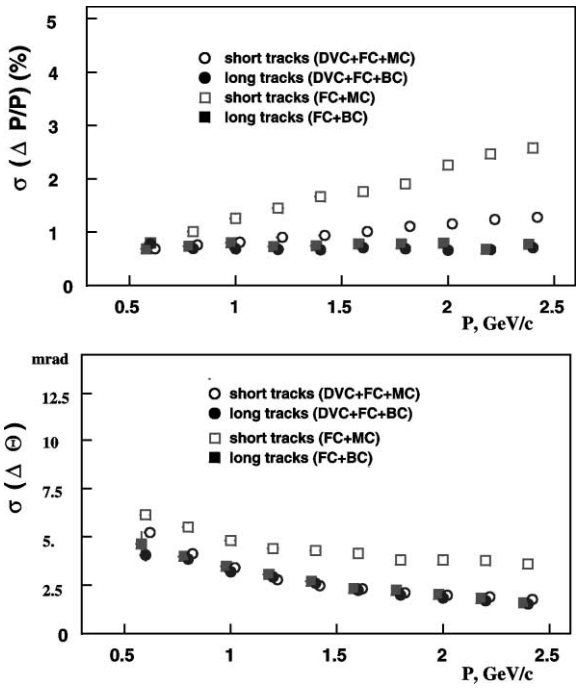

Fig. 11. Simulation results for momentum (upper panel) and angular (lower panel) resolutions versus pion momentum for short and long tracks.

The chamber efficiencies were investigated for the operating conditions of the experiment with the 1.3 T magnetic field switched on.

From the residual distributions one can conclude that a hit found in a given MC plane within the residual peaks (± 1 cm) is very likely a "real" one corresponding to the reconstructed long track. Then the chamber plane integrated efficiency has been defined as a ratio of real hits (within the

Table 4
Magnet chamber efficiencies

Chamber	U plane (%)	X plane (%)	V plane (%)
MC1-top	98.7	99.1	98.4
MC2-top	99.2	99.3	99.3
MC3-top	99.3	98.9	96.8
MC1-bottom	97.7	99.5	99.6
MC2-bottom	99.4	99.3	99.4
MC3-bottom	97.5	99.6	99.5

above mentioned spatial window) to the number of reconstructed long tracks traced through the sensitive area of a chamber.

Table 4 contains the measured efficiencies for the reconstructed events triggered by the HERMES spectrometer with particle energies larger than 3 GeV.

The efficiency measurements performed under actual running conditions confirm that the working parameters (gas composition, HV settings, PA thresholds, and signal delays) have been correctly chosen and the chamber operation is stable and reliable.

It should be noted that the overall efficiency of short track reconstruction using the front part of the HERMES tracking system and the MCs alone is nearly equal to 100% due to redundancy in the position information collected along the track. For example, it is sufficient to have hits in only 5 MC planes in order to reconstruct a short track.

In order to find out which parts of the sensitive area of the MCs result in the observed small inefficiencies, an algorithm [14] has been developed to calculate the differential (per wire) efficiency.

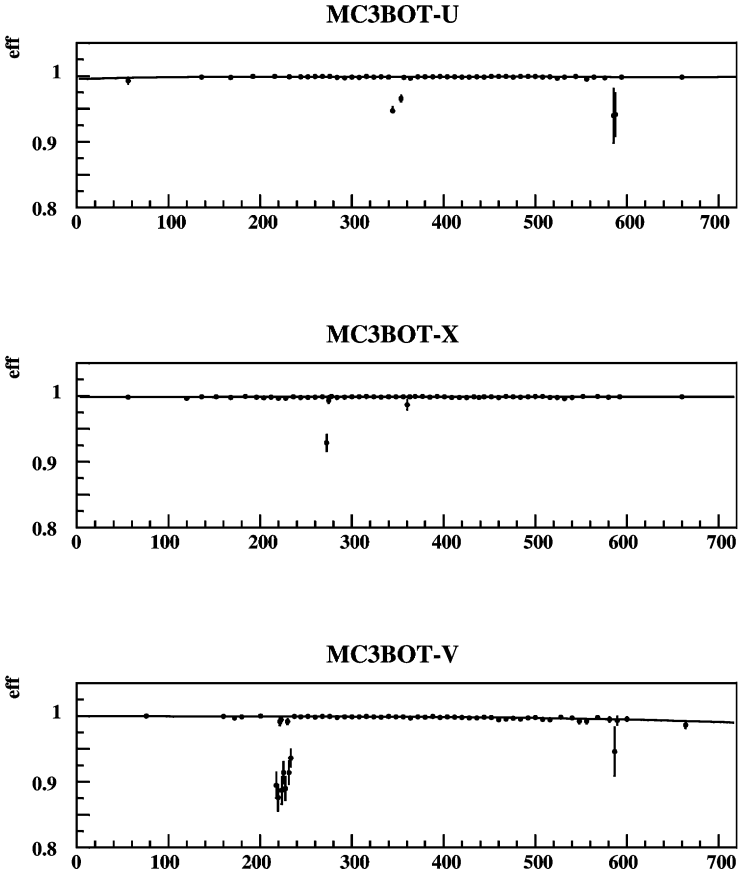

Fig. 12. Typical differential efficiencies; channels with low statistics, due to the acceptance borders, are averaged. See Ref. [14].

Definition of the efficiency per wire is basically the same as that of the integrated efficiency. The only distinction is that the differential efficiency is calculated for each wire (cell), which is specified by the location of the trace of the reconstructed track in a given cell.

Examples of the differential efficiency, measured during calibration runs in 1996–1997 with the spectrometer magnet, are shown in Fig. 12.

7. Reconstruction of Λ_0 Particles using short tracks

As was mentioned above, the MCs are of special interest due to their use in reconstructing short tracks produced by low-momentum particles which do not traverse the drift chambers in the rear part of the HERMES spectrometer. One important application is the reconstruction of the pions from $\Lambda_0(\bar{\Lambda}_0)$ decay. The invariant mass spectra obtained from short and long tracks are compared in Fig. 13. The contribution of the short tracks is very important in the analysis of reactions with Λ's, and $\bar{\Lambda}$'s in the final state, since the short tracks give better access to the part of the hadronic final state coming from the target fragmentation region. In addition, the spectrometer acceptance for Λs is much more uniform in the decay angles if short and long tracks are included rather than only long tracks; this is very helpful in the analysis of Λ polarization.

In Fig. 14 the ratio $R = (\text{short} + \text{long})/\text{long}$ is shown versus pion momentum. The ratio has been calculated using the HERMES Monte Carlo program for pions coming from Λ decay. It can be seen that the relative contribution of short tracks is considerably increased when the pion

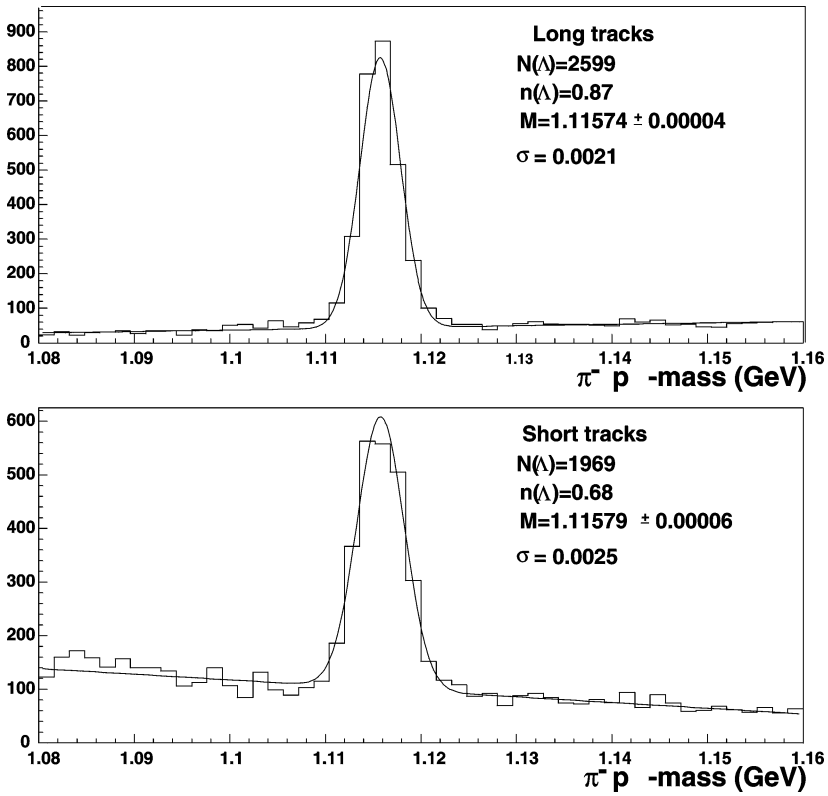

Fig. 13. The Λ_0 mass spectrum using long and short tracks. $n(\Lambda)$ is defined as the ratio of the true Λ ($N(\Lambda)$) to the total events ($N(\Lambda)$ + background) under the peak.

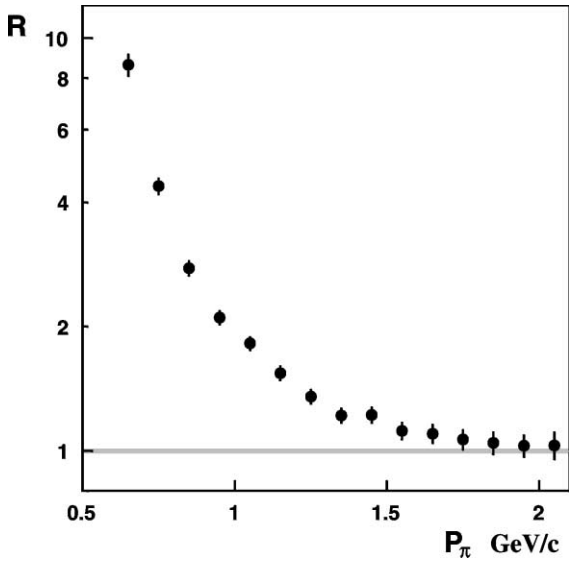

Fig. 14. The ratio R (see text) is plotted versus pion momentum for Λ-events, showing the increasing contribution of short tracks for decreasing value of momentum.

momenta are less than 1.5 GeV/c. Moreover, the contribution of short tracks reconstructed with the MCs is expected to be even more important in the study of other processes involving particles more massive than the Λ.

8. Summary

The design, construction and operation of a set of multiwire proportional chambers located in the very restricted space of the pole gap of the HERMES spectrometer magnet have been described, with special note made of the design of the mechanical frames which was necessary to ensure that the wires are kept stable and under sufficient tension. Data acquisition from the chambers is performed with the new LeCroy PCOS4 system (specially modified for HERMES) which has several advantages in comparison with similar commercial systems; among them, its compactness and reduced cabling is of particular importance for our application. Moreover, exploiting its intrinsic flexibility, we redesigned one of its components, the Backplane, making the system significantly more reliable and robust. After 5 years of operation the detector has shown satisfactory and stable performance with a tracking efficiency of 99% and a spatial resolution of 600 μm (rms) in good agreement with the design goals of the HERMES experiment.

A simulation has shown that low-momentum particles which leave the HERMES tracking system before reaching its rear drift chambers (short tracks), can only be analyzed using the MCs. Their momentum and angular resolutions are very close to the values measured for higher momentum particles which traverse all the components of the tracking system (long tracks). The capability of allowing the reconstruction of short tracks makes the MC system of special importance in the study of semi-inclusive channels where low momentum particles are involved, particularly those resulting from the decay of baryons such as the Λ_0.

Acknowledgements

This work has been partly funded by the INTAS project 93–1937.

References

[1] HERMES Collaboration, HERMES Technical Design Report, DESY–PRC 93/06.
[2] HERMES Collaboration, Nucl. Instr. and Meth. A 417 (1998) 230.
[3] G. Charpak et al., Nucl. Instr. and Meth. 62 (1968) 262; Nucl. Instr. and Meth. 80 (1970) 13.
[4] G. Charpak et al., Nucl. Instr. and Meth. 97 (1970) 377.
[5] 1996 Research Instrumentation Catalog, LeCroy Corporation Research Systems Division, LeCroy Corporation, 1996.
[6] E. Cisbani et al., The HERMES implementation of the PCOS4 system, Proceedings of the International Conference on Electronics for Particle Physics, LeCroy Research Systems, Chestnut Ridge, 28–29 May, 1997.
[7] 1993 Research Instrumentation Catalog, LeCroy Corporation Research Systems Division, LeCroy Corporation, 1993.
[8] A. Atamanchouk et al., CROS2A Coordinate Readout System, Petersburg Nuclear Physics Institute, 1993.

[9] J.D. Reid, S.V. Greene, L.E. Finch, R.D. Majka, Note on failure study of LeCroy PCOS4 2741 R/O cards, 1996.
[10] HERMES Collaboration, Phys. Lett. B 404 (1997) 383; Phys. Lett. B 442 (1998) 484; Phys. Rev. Lett. 81 (1998) 5519; Phys. Lett. B 444 (1998) 531; Phys. Rev. Lett. 82 (1999) 1164; Phys. Rev. Lett. 82 (1999) 3025; Phys. Lett. B 464 (1999) 123; hep-ex/9910071 and DESY-99-150, November 1999.
[11] T.-A. Shibata et al., Nucl. Instr. and Meth. A 411 (1998) 75.
[12] W. Wander, Ph.D. Thesis, Friedrich Alexander Universität Erlangen-Nürnberg, April 1996 (English translation: HERMES internal note 97-031).
[13] GEANT Detector Description and Simulation Tool, CERN Program Library, Long Writeup, W5013, 1994.
[14] Yu. Naryskin, S. Belostotski, O. Grebenyuk, O. Miklukho, Magnet chambers efficiencies, HERMES Internal Note 98-013, April 1998.